AKTA KIMIA
INDONESIA

Akta Kimindo Vol. 10(1), 2025: 69-81

Compositional and Thermal Effects on the Phase Stability and Crystallinity of Cu_2SnS_3 Nanoparticles

Agus Ismail[1*], Destia Nurika[2], Agus Wismogroho[2], Ikhlasul Amal[2]

[1] *Industrial Engineering, Universitas Mercu Buana, DK Jakarta, Indonesia 11650*
[2] *Research Center Nanotechnology System, National Research and Innovation Agency, Kawasan Sains dan Teknologi Serpong, Tangerang Selatan, Indonesia 15314*

** Email: agus.ismail@mercubuana.ac.id*

Abstract

Cu_2SnS_3 (CTS) is a promising semiconductor for photovoltaic applications, yet its synthesis via solid-state sintering remains insufficiently explored. This study examines the phase evolution and structural properties of CTS thin films fabricated from Cu, Sn, and S elemental precursors sintered at 300 °C, 400 °C, 500 °C, and 600 °C. X-ray diffraction (XRD) analysis confirmed that stoichiometric CTS attained optimal phase purity at 500°C, whereas off-stoichiometric compositions resulted in secondary phases such as Cu_2S, $Cu_{9.67}Sn_{2.33}S_{13}$, and SnS_2. Scanning electron microscopy (SEM) revealed microstructural transformations, with well-defined crystalline domains emerging at 500°C but excessive grain coalescence in Cu-rich samples. Energy-dispersive X-ray spectroscopy (EDX) verified compositional variations, underscoring the critical role of stoichiometry in phase stability. These findings demonstrate that precise compositional control and optimized sintering conditions are essential for high-purity CTS films, advancing their potential for enhanced photovoltaic performance and long-term operational stability.

Keyword: *Cu_2SnS_3, solid-state sintering, phase purity, photovoltaic, thin films*

Abstrak

Cu_2SnS_3 (CTS) adalah semikonduktor yang menjanjikan untuk aplikasi fotovoltaik, namun sintesis CTS melalui sintering zat padat belum banyak penelitian yang melakukannya. Pada studi ini meneliti evolusi fasa dan sifat struktur dari CTS lapisan tipis yang dibuat dari precursor unsur Cu, Sn dan S yang disinter pada suhu 300 °C, 400 °C, 500 °C, dan 600 °C. Analisis difraksi sinar X (XRD) mengkonfirmasi bahwa CTS dengan kondisi stoikiometri mencapai kemurnian fasa yang optimal pada suhu 500 °C, sedangkan komposisi yang tidak stoikiometri menghasilkan fasa sekunder seperti Cu_2S, $Cu_{9.67}Sn_{2.33}S_{13}$,

dan SnS_2. Analisis SEM (scanning electron microscope) mengungkap transformasi mikrostruktur dengan domain kristal terdefinisi dengan baik muncul pada suhu 500 °C, tetapi koalesensi butiran yang berlebihan dalam sampel yang kaya dengan unsur Cu. Dengan EDX (Energy-dispersive X-ray spectroscopy) memverifikasi variasi komposisi yang menggarisbawahi peran penting stoikiometri dalam kestabilan fasa. Temuan ini menunjukkan bahwa kontrol komposisi yang tepat dan kondisi sintering yang dioptimalkan sangat penting untuk film CTS dengan kemurnian tinggi, meningkatkan potensinya untuk meningkatkan kinerja fotovoltaik dan stabilitas operasional jangka panjang.

***Kata Kunci**: Cu_2SnS_3, sintering zat padat, kemurnian fasa, fotovoltaik, lapisan tipis*

I. INTRODUCTION

Cu_2SnS_3 (CTS) is a promising semiconductor owing to its optimal band gap of approximately 1 eV, a respectable Hall mobility of 1.79 $cm^2 \cdot V^{-1} \cdot s^{-1}$, and a high carrier concentration of 1.85×10^{20} cm^{-3} [1–3]. Moreover, its tuneable band gap—ranging from 1.1 to 1.5 eV—enhances its suitability as a photovoltaic absorber [4]. Recently, CTS has garnered significant interest as a ternary nanomaterial because controlling the stoichiometric ratios of its constituent elements is more straightforward than in more complex quaternary semiconductors [5]. In addition to its low cost and non-toxicity, these attributes make CTS attractive for sustainable, large-scale applications [6]. Various polymorphs of CTS have been investigated for applications in optoelectronics [7], sensors [8], solar cell absorber layers [9], and thermoelectric devices [10]. Consequently, CTS is emerging as a compelling alternative for solar cell photo-absorbing layers, with CTS-based devices achieving a maximum efficiency of 4.63% [11, 12].

The synthesis of CTS nanoparticle thin films through a hybrid approach combining chemical and physical methods remains underexplored. Existing methodologies include solid-state reactions in sulphur vapour at 530°C for 6 hours, followed by the sequential deposition of copper and tin layers [13]. Chemical vapour deposition (CVD) techniques, such as aerosol-assisted CVD (AACVD), involve the atomization of an $SnCl_4$ and $CuCl_2$ solution, which is sprayed onto heated alkali-free glass substrates at 390°C [14]. Additionally, physical vapour deposition (PVD) methods, such as electron beam evaporation followed by sulfurization in an H_2S atmosphere at varying temperatures and durations, have been employed [15]. The integration of these chemical and physical deposition techniques presents a promising

strategy for advancing CTS-based photovoltaic technologies, offering potential improvements in efficiency, cost-effectiveness, and environmental stability [15].

Despite notable progress in deposition techniques, the challenges associated with sintering remain a significant concern, particularly regarding the long-term stability of CTS nanoparticles (NPs). Under practical operating conditions—including electrical stress, chemical exposure, and thermal fluctuations—CTS NPs are prone to degradation due to sintering effects [16]. However, this aspect has received limited attention in research.

Despite the promise of CTS, achieving phase-pure materials via scalable, cost-effective solid-state sintering from elemental precursors remains a significant challenge, often leading to undesirable secondary phases and impacting long-term device stability. To overcome this, our research provides a novel and systematic investigation into the effects of both annealing temperature and precursor stoichiometry on the phase evolution and structural properties of Cu_2SnS_3 thin films. By precisely mapping the conditions that yield optimal phase purity and crystallinity, while identifying the mechanisms behind off-stoichiometric impurity formation, this study offers critical advancements towards the reliable synthesis of high-quality CTS for photovoltaic applications.

This study focuses on the synthesis of Cu_2SnS_3 nanoparticles using a solid-state sintering method, wherein particles bond and solidify under heat application below the material's melting point. This process typically enhances density, mechanical strength, and electrical and thermal conductivity, even as surface area decreases, often without substantial changes in overall density [18].

The primary objective of this study is to determine the optimal experimental conditions for synthesizing CTS compounds via solid-state sintering. This technique involves annealing CTS from elemental powders of Cu, Sn, and S at elevated temperatures. The structural properties of the resulting films were analysed using X-ray diffraction (XRD) to assess phase composition and crystallinity. Additionally, scanning electron microscopy (SEM) and energy-dispersive X-ray spectroscopy (EDX) were employed to investigate surface morphology and elemental composition.

II. EXPERIMENTAL DETAILS

2.1. Materials

Copper (Cu), tin (Sn), and sulfur (S) powders were used as raw materials for CTS synthesis. These powders were weighed in

stoichiometric proportions to achieve the desired composition.

2.2. Sample Preparation

Commercially available elemental powders of Cu, Sn, and S were weighed to prepare mixed powders with varying Cu:Sn:S ratios, including a stoichiometric composition, a Cu-rich variation, and a Cu-poor variation. The compositions were as follows:

- Stoichiometric composition: Cu2SnS3 (2:1:3 w/w)
- Cu-rich variation: 2.2:0.8:3 w/w
- Cu-poor variation: 1.8:1.2:3 w/w

The mixed powders, along with stainless steel balls, were placed in a stainless-steel container inside an argon-filled glove box. The ball-to-powder weight ratio (BPR) was maintained at 10:1. High-energy milling (HEM) was performed using a HEM-3D instrument (designed by BRIN) at 1200 rpm, with a cycle of 30 minutes of milling followed by 5 minutes of rest. The resulting powder mixture was then compacted into pellets for further processing

2.3. Sintering Process

The sintering process involves heating the compressed material to a temperature below its melting point, allowing the particles to bond and form a solid mass. In this study, sintering was carried out at various temperatures: 300 °C, 400 °C, 500 °C, and 600 °C. This specific temperature range was chosen based on prior research on Cu_2SnS_3 synthesis [19] and is widely recognized as optimal for achieving phase-pure kesterite-type compounds [20, 21]. To prevent contamination from atmospheric gases, the pellets were placed inside evacuated ampoule tubes before sintering. The sintering conditions included of temperature ramp rate of 50 °C/min and a holding time for 2 hours.

2.4. Characterization Techniques

The surface and cross-sectional morphologies of the sintered films were analysed using scanning electron microscopy (SEM; Model: JEOL JSM-IT200). The influence of sulfurization temperatures on the crystallinity of CTS thin films was investigated using high-resolution X-ray diffraction (XRD; SMARTLAB RIGAKU). The XRD measurements were conducted over a 2θ range of 10°–90°, with a scan speed of 5°/min and a step width of 0.01°, using Cu-Kα radiation (operated at 30 mA and 40 kV). Phase identification was performed using HighScore Match software.

III. RESULT AND DISCUSSION

The X-ray diffraction (XRD) patterns of Cu-poor, Cu-rich, and stoichiometric Cu_2SnS_3 (CTS) samples synthesized at varying

sintering temperatures (400°C to 600°C) are presented in Fig. 1A-D. These patterns were analyzed to identify the crystalline phases and assess the impact of composition and temperature on phase evolution. For Cu-poor samples (Fig. 1A), the primary CTS peak at ~48° shows weak intensity at 500°C, suggesting incomplete crystallization, while additional characteristic CTS peaks at ~53° and ~59° are present across all temperatures. Critically, at 600°C, a distinct SnS_2 phase emerges, indicating its thermodynamic favorability at elevated sintering temperatures under Cu-deficient conditions. This can be attributed to the limited availability of Cu in Cu-poor compositions, which shifts the thermodynamic equilibrium toward the formation of tin-rich secondary phases such as SnS_2. The presence of SnS_2 is undesirable for solar absorber applications, as it introduces recombination centers that degrade charge carrier transport and overall device efficiency. In contrast, Cu-rich samples (Fig. 1B) show characteristic peaks at ~28°, ~32°, ~48°, ~53°, and ~59° with increasing intensities at 500°C, indicating enhanced crystallinity due to improved atomic diffusion at elevated temperatures. However, at 600°C, the desired CTS peaks diminish significantly, concomitant with the detrimental formation of Cu_2S and $Cu_{9.67}Sn_{2.33}S_{13}$ secondary phases. The formation of Cu_2S arises from the excess Cu in the system, which reacts with sulfur to form this copper sulfide phase. Similarly, the $Cu_{9.67}Sn_{2.33}S_{13}$ phase likely forms due to the segregation of Cu and Sn atoms under high-temperature conditions, leading to non-stoichiometric clustering. These secondary phases are detrimental to the performance of CTS as a solar absorber, as they create heterogeneities in the material and reduce its optical absorption efficiency. For stoichiometric samples (Fig. 1C), a significant phase evolution toward purity is observed. The peak at ~33°, likely corresponding to a minor impurity or amorphous phase, disappears above 400 °C. While the main CTS peak at ~48° persists across all temperatures, its broadening at 500 °C may suggest slight variations in crystallite size or lattice strain. Crucially, other impurity peaks (e.g., at ~32°, ~53°, and ~59°), along with the SnS_2 phase detected at lower temperatures, completely vanish at 500 °C, unequivocally demonstrating optimal phase purity and successful CTS formation at this intermediate sintering temperature. This behavior aligns with prior studies reporting optimal crystallinity under specific thermal conditions, where the balance between Cu and Sn promotes the formation of pure CTS without secondary phases. At 400 °C (Fig. 1D), the diffraction patterns reveal that the peak at ~48° is present in all samples, with its

intensity notably higher in the $Cu_{1.8}Sn_{1.2}S_3$ sample. This suggests that slight deviations from stoichiometry, such as a Cu-rich composition, enhance the crystallinity of the CTS phase. Peaks at ~32° and ~53° are also observed consistently, while the SnS_2 phase is only detected in the Cu_2SnS_3 sample, underscoring the influence of composition on phase stability. These findings demonstrate that both composition and sintering temperature significantly affect the structural properties of CTS. From a thermodynamic perspective, the formation of secondary phases such as SnS_2, Cu_2S, and $Cu_{9.67}Sn_{2.33}S_{13}$ is driven by the imbalance of Cu and Sn in the precursor mixtures, which alters the Gibbs free energy landscape during synthesis. Kinetic factors, such as diffusion rates and reaction times, also play a critical role, particularly at higher temperatures where rapid atomic rearrangements can lead to phase segregation.

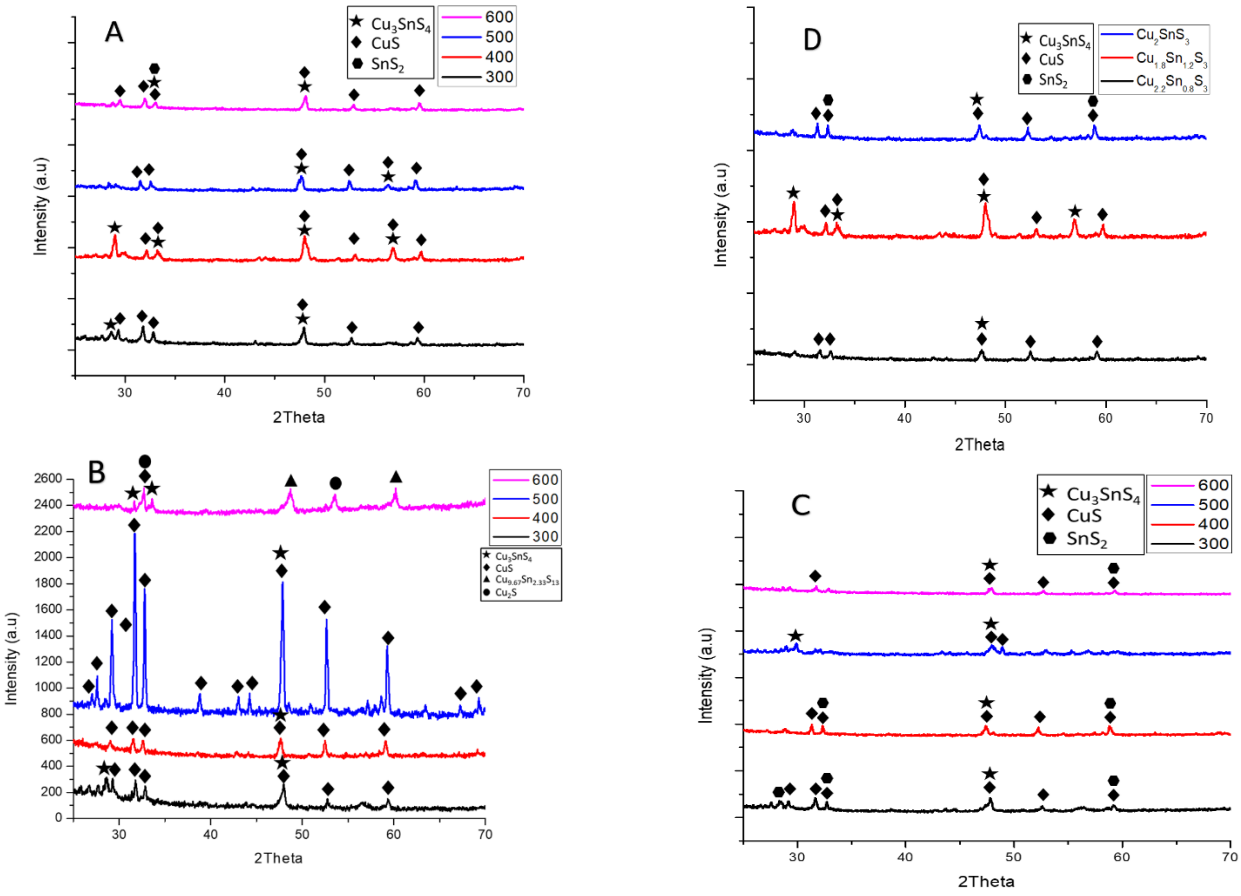

Fig 1. A. Cu Poor, B. Cu Rich, C. Cu Stoikiometri, D. Temperature 400 ^{0}C

From an application standpoint, the presence of secondary phases not only reduces the optical and electrical quality of CTS but also introduces interfaces that act as recombination centers, limiting the material's performance as a solar absorber. Therefore, optimizing the synthesis conditions—particularly achieving near-stoichiometric compositions and controlling sintering temperatures—is crucial for obtaining high-quality CTS with minimal secondary phases.

The surface morphology of semiconductor materials plays a critical role in their optoelectronic performance, as it directly influences properties such as light absorption, charge carrier transport, and interfacial interactions. Figure 2a-f presents SEM images of CTS nanoparticles (NPs) at 1000x magnification, revealing distinct morphological variations influenced by both sintering temperature and composition. At 300 °C under stoichiometric Cu conditions, the particles exhibit a non-uniform granular morphology with a rough surface, indicative of incomplete crystallization or insufficient atomic diffusion at this relatively low temperature. As the temperature increases to 400 °C, the particles begin to adopt a more defined structure, appearing as slabs with some degree of agglomeration. By 500 °C, the morphology transitions to a more regular granular structure with a smoother surface, suggesting improved crystallinity and reduced surface defects due to enhanced thermal energy facilitating atomic rearrangement. At 600 °C under stoichiometric Cu conditions, the particles evolve into a plate-like morphology with a smooth surface, which is consistent with prior studies reporting the formation of well-defined structures at higher temperatures. Variations in composition further highlight the sensitivity of morphology to Cu content. Under Cu-poor conditions at 600 °C (Fig. 2e), the particles form a lamellar-like or plate-like structure. This open surface morphology, distinct from stoichiometric samples, further supports the XRD observation of SnS_2 secondary phase formation (Fig. 1A), as the limited Cu availability likely prevents dense packing of the desired CTS phase. In contrast, under Cu-rich conditions at 600 °C, the particles display significant agglomeration with a coarse granular morphology. This agglomeration can be attributed to the high surface energy associated with smaller particle sizes, as reported in previous studies [12]. The excess Cu in the system likely enhances particle coalescence, consistent with the formation of Cu_2S and $Cu_{9.67}Sn_{2.33}S_{13}$ observed in XRD (Fig. 1B), leading to larger clusters and irregular morphologies that are detrimental to film quality. In addition to these observations, crystallites and randomly oriented particles

are also visible across the samples. Notably, agglomeration is more pronounced at lower temperatures (300 °C and 500 °C) for stoichiometric Cu compositions, as well as at 600 °C for Cu-rich compositions. This trend suggests that both temperature and Cu content influence particle growth kinetics, with higher temperatures and Cu excess promoting particle aggregation due to increased surface energy and diffusion rates. These morphological characteristics have important implications for the material's optoelectronic properties, as agglomeration and irregular surface features can introduce defects and scattering centers, potentially reducing the efficiency of charge carrier transport and light absorption.

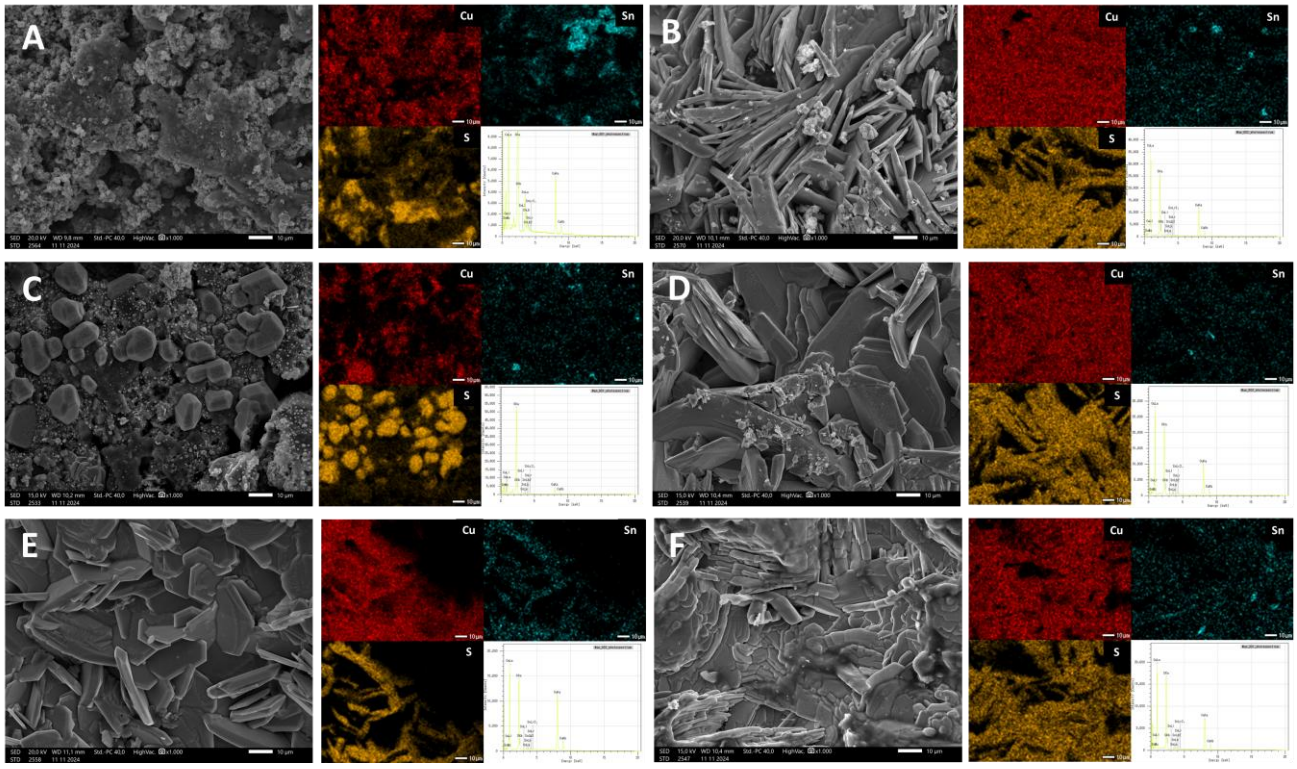

Fig 2.SEM images of CTS thin films A. Cu-Stoichiometry T300 °C, B. T400 °C, C. T500 °C, D. T600 °C, E. Cu-Poor T600 °C, F. Cu-Rich T600 °C

Figure 2 also presents EDX and SEM-EDS elemental mapping data, where the colors in the mapping indicate the distribution of compounds within the sample. The red regions correspond to copper (Cu), the blue regions to tin (Sn), and the gold regions to sulfur (S). These mappings provide insights into the elemental composition and spatial distribution of Cu, Sn, and S across the synthesized CTS samples under various thermal treatment and composition conditions. The EDX spectra reveal the dominance of Cu, Sn, and S elements in the samples, with their relative intensities varying depending on the sintering temperature and composition. At 300 °C under stoichiometric conditions (Fig. 2, EDX map corresponding to 2a), the EDX spectra show significant peaks for Cu, Sn, and oxygen (O). The presence of oxygen likely indicates residual precursors or partial oxidation in the initial formation stages, while the relatively uniform distribution of Cu, Sn, and S suggests early-stage elemental mixing prior to complete crystallization. At 400 °C under stoichiometric conditions, the intensities of Cu and Sn increase relative to O, suggesting a phase transformation or enhanced crystallinity as the material undergoes further thermal processing. This reduction in oxygen content indicates the decomposition of oxide phases and the gradual formation of pure CTS. At 500 °C, the peaks for Cu and Sn become even more pronounced, signifying the stabilization of a more crystalline and thermally robust phase. This elemental distribution homogeneity at 500 °C strongly corroborates the optimal phase purity observed in XRD at this temperature (Fig. 1C). This trend underscores the role of higher temperatures in promoting atomic rearrangement and reducing structural defects. At 600 °C under stoichiometric conditions, the intensities of Cu, Sn, and S reach their highest levels, reflecting the formation of a well-defined and highly crystalline CTS phase. The minimal presence of oxygen at this temperature suggests near-complete conversion of precursor materials into the desired compound. In contrast, under Cu-poor conditions at 600 °C (Fig. 2, EDX map corresponding to 2e), the EDX mapping clearly shows regions with significantly lower Cu intensity relative to Sn and S. This elemental deficiency visually supports the XRD observation of SnS_2 secondary phase formation (Fig. 1A), where the lack of available copper drives the formation of tin-rich impurities. Conversely, under Cu-rich conditions at 600 °C, the intensity of Cu increases substantially, highlighting an excess of copper. The EDX mapping further reveals distinct regions of Cu-rich elemental segregation, providing direct spatial evidence

for the formation of non-stoichiometric phases like Cu_2S or $Cu_{9.67}Sn_{2.33}S_{13}$, as definitively identified by XRD (Fig. 1B). These compositional imbalances can significantly alter the material's crystal structure and optoelectronic properties.

Overall, these findings demonstrate that both temperature and composition variations play a critical role in determining the elemental distribution, crystallinity, and phase purity of the material. The EDX and SEM-EDS results corroborate the XRD observations, emphasizing the importance of optimizing synthesis conditions to achieve high-quality CTS with minimal secondary phases and optimal stoichiometry. Such optimization is essential for enhancing the material's performance in optoelectronic applications, particularly as a solar absorber.

IV. CONCLUSSION

This study demonstrates that the structural and morphological properties of Cu_2SnS_3 (CTS) are significantly influenced by sintering temperature and composition. XRD analysis revealed that stoichiometric CTS achieves optimal crystallinity at 500 °C, effectively minimizing secondary phases such as SnS_2, Cu_2S, and $Cu_{9.67}Sn_{2.33}S_{13}$, which can degrade optoelectronic performance. SEM and EDX mapping confirmed that Cu-rich compositions promote agglomeration, whereas Cu-poor conditions lead to the formation of tin-rich phases, both of which compromise film uniformity and structural integrity. These findings underscore the critical role of stoichiometric control and thermal treatment in achieving high-purity CTS for solar absorber applications.

Given the impact of composition-dependent phase evolution, future research should focus on refining sintering parameters to enhance phase stability, exploring doping strategies to stabilize the CTS phase, and evaluating its electrical properties to improve photovoltaic performance. Additionally, alternative synthesis approaches, such as combinatorial deposition techniques, could further optimize the material's efficiency and scalability for next-generation thin-film solar cells.

Cu_2SnS_3 (CTS) is a promising semiconductor material with a tunable band gap suitable for photovoltaic applications. Despite its advantages, the synthesis of CTS thin films using a solid-state sintering method remains underexplored. This study investigates the synthesis and characterization of CTS thin films prepared from Cu, Sn, and S elemental powders through a solid-state sintering process. The sintering was conducted at varying temperatures (300 °C, 400 °C, 500 °C, and 600 °C) to determine the

optimal conditions for phase purity and crystallinity. X-ray diffraction analysis revealed that stoichiometric CTS exhibited improved phase purity at 500°C, whereas Cu-rich and Cu-poor samples formed undesirable secondary phases such as Cu_2S, $Cu_{9.67}Sn_{2.33}S_{13}$, and SnS_2 at elevated temperatures. Scanning electron microscopy showed morphological transformations from irregular granules at 300 °C to well-defined structures at 500 °C, with excessive agglomeration occurring in Cu-rich samples. Energy-dispersive X-ray spectroscopy confirmed compositional variations, highlighting the significance of stoichiometry in achieving phase-pure CTS. The results indicate that maintaining a balanced Cu:Sn:S ratio and optimizing sintering temperature are crucial to preventing secondary phase formation and enhancing material quality. These findings contribute to the advancement of CTS-based solar absorber materials by identifying critical synthesis parameters that impact structural and morphological properties. Optimized CTS films can potentially improve photovoltaic efficiency and long-term stability, making them suitable for sustainable energy applications. Future work should focus on refining synthesis techniques to further enhance material performance.

ACKNOWLEDGEMENT

The authors would like to express gratitude to Korea Institute of Technology School Partnership Project for their research grant

DAFTAR PUSTAKA

[1] X. Liang, Q. Cai, W. Xiang, Z. Chen, J. Zhong, Y. Wang, M. Shao, Z. Li, J. Mater. Sci. Technol., vol. 29, pp. 231–236, (2013); https://doi.org/10.1016/j.jmst.2012.12.011

[2] B. Li, Y. Xie, J. Huang, Y. Qian, J. Solid State Chem., vol. 153, pp. 170–173, (2000); https://doi.org/10.1006/jssc.2000.8772

[3] C. Wu, Z. Hu, C. Wang, H. Sheng, J. Yang, Y. Xie, Appl. Phys. Lett., vol. 91, pp. 143104, (2007); https://doi.org/10.1063/1.2790491

[4] A. Lokhande, et al., J. Alloys Compd., vol. 656, pp. 295–310, (2016); https://doi.org/10.1016/j.jallcom.2015.09.232

[5] A. Kanai, et al., Jpn. J. Appl. Phys., vol. 54(8S1), pp. 08KC06, (2015); 10.7567/JJAP.54.08KC06

[6] H. Nautiyal, K. Lohani, B. Mukherjee, E. Isotta, M. A. Malaguti, N. Ataollahi, N., Pallecchi, I., Putti, M., Misture, S.T., Rebuffi, L. and P. Scardi,

Nanomaterials, vol. 13(2), pp. 366, (2023); https://doi.org/10.3390/nano13020366

[7] S.B. Jathar, S.R. Rondiya, Y.A. Jadhav, D.S. Nilegave, R.W. Cross, S.V. Barma, M.P. Nasane, S.A. Gaware, B.R. Bade, S.R. Jadkar, et al., Chem. Mater., vol. 33, pp. 1983–1993, (2021); https://doi.org/10.1016/j.jallcom.2017.03.135

[8] A.C. Lokhande, A.A. Yadav, J.Y. Lee, M. He, S.J. Patil, V.C. Lokhande, C.D. Lokhande, J.H. Kim, J. Alloys Compd., vol. 709, pp. 92–103, (2017); https://doi.org/10.1016/j.jallcom.2017.03.135

[9] A.S. Mathur, S. Upadhyay, P.P. Singh, B. Sharma, P. Arora, V.K. Rajput, P. Kumar, D. Singh, B.P. Singh, Opt. Mater., vol. 119, pp. 111314, (2021); https://doi.org/10.1016/j.optmat.2021.111314

[10] Q. Tan, W. Sun, Z. Li, J.F. Li, J. Alloys Compd., vol. 672, pp. 558–563, (2016); https://doi.org/10.1016/j.jallcom.2016.02.185

[11] S. Rahaman, M.K. Singha, M.A. Sunil, K. Ghosh, Superlattice Microstruct., vol. 145, pp. 1–10, (2020); https://doi.org/10.1016/j.spmi.2020.106589

[12] A. Kanai, M. Sugiyama, Sol. Energy Mater. Sol. Cells, vol. 231, pp. 1–10, (2021); https://doi.org/10.1016/j.solmat.2021.111315

[13] M. Bouaziz, J. Ouerfelli, S.K. Srivastava, J.C. Bernède, M. Amlouk, Vacuum, vol. 85(8), pp. 783–786, (2011); https://doi.org/10.1016/j.vacuum.2010.10.001

[14] K. Tanaka, M. Kowata, F. Yoshihisa, S. Imai, W. Yamazaki, Thin Solid Films, vol. 697, pp. 137820, (2020); https://doi.org/10.1016/j.tsf.2020.137820

[15] Z. Tang, K. Kosaka, H. Uegaki, J. Chantana, Y. Nukui, D. Hironiwa, T. Minemoto, Phys. Status Solidi A, vol. 212, pp. 2289–2296, (2015); https://doi.org/10.1002/pssa.201532121

[16] X. Chen, C. Li, B. Li, Y. Ying, S. Ye, D.N. Zakharov, G. Zhou, ACS Nano, vol. 18(45), pp. 31160–31173, (2024); https://doi.org/10.1021/acsnano.4c09056

[17] D.L. Johnson, in: Concise Encyclopedia of Advanced Ceramic Materials, Pergamon, pp. 454–458, (1991); https://10.1016/0921-5093(93)90458-q

[18] Y. Li, H. Sun, J. Song, Z. Zhang, H. Lan, L. Tian, K. Xie, Materials, vol. 16(5), pp. 2019, (2023);

https://doi.org/10.3390/ma16052019

[19] Gu, W., Liu, B., Li, S. et al. Phase evolution and thermoelectric performance of Cu2SnS3. J Mater Sci: Mater Electron 34, 1096 (2023). https://doi.org/10.1007/s10854-023-10530-7

[20] Kim, KH., Amal, I. Growth of Cu2ZnSnSe4 thin films by selenization of sputtered single-layered Cu-Zn-Sn metallic precursors from a Cu-Zn-Sn alloy target. Electron. Mater. Lett. 7, 225–230 (2011). https://doi.org/10.1007/s13391-011-0909-x

[21] Amal, I., Kim, KH. Crystallization of kesterite Cu_2ZnSnS_4 prepared by the sulfurization of sputtered Cu–Zn–Sn precursors Thin Solid Films Volume 534, 1 May 2013, Pages 144-148. https://doi.org/10.1016/j.tsf.2013.02.028